

# Simulation of Turbulent Diffusion and Reactive Flows by the PDF Methods

Yasuhiko SAKAI\*<sup>1</sup>, Takashi KUBO\*<sup>1,\*2</sup> and Haruki SUZUKI\*<sup>1</sup>

\*1 : Department of Mechano-Informatics & Systems, Nagoya University,  
Furo-cho, Chikusa-ku, Nagoya 464-8603, Japan

\*2 (present) : Hitachi, Ltd, Mechanical Engineering Research Laboratory,  
502, Kandatsu-cho, Tsuchiura, Ibaraki 300-0013, Japan

## 1 Introduction

Turbulent diffusion of matter and mixing phenomena with the chemical reaction are practically important in connection with many engineering and environmental problems. If the experiments for some specific turbulent diffusion or reactive flow phenomena would be planned, it apparently needs very hard labor and a lot of cost. On the other hand, the numerical simulations by computers have become effective to predict these phenomena because of the improvement of computers and the development of numerical methods. Generally, there are Eulerian and Lagrangian methods for the simulation of the turbulent diffusion field. In the present study, we adopted the Lagrangian PDF (Probability Density Function) method (Pope, 1985, 1994; Dopazo, 1994) which is a kind of Monte-Carlo method. In the Lagrangian PDF method, the exact velocity-scalar joint PDF is approximated by the discrete PDF for a set of many stochastic particles, and the variations of velocity and scalar are modeled by the Lagrangian equation (See Pope, 1985, 1994; Dopazo, 1994, for details of the method).

In this study, the following two fundamental problems of turbulent diffusion and reactive flows have been investigated.

(A) The reactive-scalar mixing layer in a grid-generated turbulence

(B) The axisymmetric point source plume diffusion in a turbulent pipe flow

The first problem (A) has been studied experimentally by Bilger et al. (1991) for the gas phase and Komori et al. (1993, 1994) for the liquid phase. Since the PDF method has been mainly developed in the combustion engineering, there are still only a limited number of researches in the liquid phase (e.g. Pipino and Fox, 1994; Tsai and Fox, 1994). For this reason, we pay attention on the liquid phase reaction in the first problem (A). About the simulation of this problem, Komori et al. (1991) also proposed a stochastic two particle model, but in their model, it was assumed that the chemical reaction occurs when the distance between two particles becomes smaller than the Kolmogorov scale. Recently, Bilger (1993) and Klimenko (1990) have independently developed the conditional moment closure (CMC) model. In the CMC method, the information of mixture fraction is indispensable to get the unconditional statistics of the flow, and the Lagrangian PDF method is useful to predict the mixture fraction. In this study, to solve the first problem, the simplified Langevin model (Pope, 1985) is used for the velocity of stochastic particles. For the molecular mixing, three models: the Curl's model (Curl, 1963), the modified Curl's model (Dopazo, 1979; Janicka et al., 1979; Pope, 1982), and the binomial Langevin model (Valiño and Dopazo, 1991) are adopted. The results are compared with the experimental data in liquid phase (Komori et al., 1993, 1994).

With regard to the second problem (B), as the velocity model of the stochastic particles, a generalized Langevin model expressed in the cylindrical coordinate system is adopted. The generalized Langevin model was first proposed by Haworth and Pope (1986) and expressed in the cylindrical coordinate system by Sakai et al. (1999). This model is constructed to satisfy the consistency condition of velocity field (Pope, 1987) and thermodynamic constraint (Sawford, 1986). On the other hand, as the molecular mixing model, two models (i.e. the Dopazo's deterministic model (Dopazo, 1975) and the modified Curl's model (Dopazo, 1979; Janicka et al., 1979; Pope, 1982)) are attempted. In this study, the scalar diffusion field from the point source at the center of the pipe is simulated and compared with experimental data by Becker et al. (1966).

This paper is structured as follows: In the following Section, we recall the Lagrangian PDF method as developed by Pope (1985), (1994) and by Dopazo (1994), and give the simulation results of the reactive-scalar mixing layer in the grid-turbulence of the liquid phase (Problem(A)). In Section 3, the simulation models and results of axisymmetric point source plume in a fully developed turbulent pipe flow (Problem (B)) are given. In both Section 2 and 3, the effectiveness of the molecular mixing models used in this study is evaluated by comparing the simulation results with the experimental data. In the last Section, we summarize the content of this paper and make some remarks about our future works by the Lagrangian PDF method.

## 2 Reactive-Scalar Mixing Layer in Grid-Turbulence (Problem (A))

### 2.1 Simulation Method

#### 2.1.1 PDF Transport Equation

The transport equation for the velocity-scalar joint PDF  $f(\mathbf{V}, \psi; \mathbf{x}, t)$  in incompressible flow (Pope, 1985) is given by

$$\begin{aligned} \frac{\partial f}{\partial t} + V_j \frac{\partial f}{\partial x_j} - \frac{1}{\rho} \frac{\partial \langle p \rangle}{\partial x_j} \frac{\partial f}{\partial V_j} + \frac{\partial}{\partial \psi_\alpha} (w_\alpha f) \\ = \frac{1}{\rho} \frac{\partial}{\partial V_j} \left[ \left\langle -\frac{\partial \tau_{ij}}{\partial x_i} + \frac{\partial p'}{\partial x_j} \middle| \mathbf{V}, \psi \right\rangle f \right] \\ + \frac{\partial}{\partial \psi_\alpha} \left[ \left\langle \frac{\partial J_i^\alpha}{\partial x_i} \middle| \mathbf{V}, \psi \right\rangle f \right], \end{aligned} \quad (1)$$

where  $\mathbf{V}$  and  $\psi$  are sample spaces corresponding to the velocity  $\mathbf{U}$  and the concentration  $\Gamma$ , respectively, and  $\mathbf{x}$  is the position in the physical space,  $t$  is the time,  $\rho$  is the density,  $p$  is the pressure,  $w_\alpha$  is the chemical source term for species  $\alpha$ ,  $\tau_{ij}$  is the viscous stress tensor, and  $J_i^\alpha$  is the diffusive flux vector for species  $\alpha$ .  $\langle Q | \mathbf{V}, \psi \rangle$  stands for the conditional expectation of  $Q$ , given that  $\mathbf{U}(\mathbf{x}, t) = \mathbf{V}$  and  $\Gamma(\mathbf{x}, t) = \psi$ , where  $Q = Q(\mathbf{U}, \Gamma)$  is a function of  $\mathbf{U}$  and  $\Gamma$ .

The terms on the left-hand side of Eq.(1) represent the unsteady term, the transport in the physical space, the transport in the velocity space by the mean pressure gradient, and the transport in the scalar space by the reaction, respectively. All these terms can be treated without approximation. The terms on the right-hand side of Eq.(1) stand for the transport in the velocity space by the viscous stress and by the fluctuating pressure gradient and the transport in the scalar space by the molecular fluxes. These terms including conditional expectations must be modeled.

In the Lagrangian PDF method, the velocity-scalar joint PDF within the solution domain,  $f(\mathbf{V}, \psi; \mathbf{x}, t)$ , is approximated by  $N(t)$  stochastic particles. The state of the  $n$ th stochastic

particle at time  $t$  is represented by

$$\mathbf{U}^{(n)}(t), \mathbf{\Gamma}^{(n)}(t), \mathbf{x}^{(n)}(t) \quad (n = 1, 2, \dots, N(t)). \quad (2)$$

The discrete PDF of the stochastic particle is defined by

$$f_N(\mathbf{V}, \boldsymbol{\psi}; \mathbf{x}, t) = \frac{1}{N} \sum_{n=1}^N \delta(\mathbf{V} - \mathbf{U}^{(n)}) \delta(\boldsymbol{\psi} - \mathbf{\Gamma}^{(n)}) \delta(\mathbf{x} - \mathbf{x}^{(n)}), \quad (3)$$

and the relation between the discrete PDF  $f_N$  and the true PDF  $f$  is

$$f(\mathbf{V}, \boldsymbol{\psi}; \mathbf{x}, t) = \langle f_N(\mathbf{V}, \boldsymbol{\psi}; \mathbf{x}, t) \rangle, \quad (4)$$

i.e., the expectation of the discrete PDF is the true PDF (Pope, 1985).

The modeled joint PDF equation is solved numerically by integrating the state of the stochastic particles under the given initial and boundary conditions. The Lagrangian PDF simulation is one of the Monte Carlo methods. In the following, the models of the velocity and concentration of the stochastic particles used in the Problem (A) are given.

### 2.1.2 Velocity

Since the mixing layer in a grid-generated turbulence is considered in this study, the velocity of the stochastic particle is modeled by the following simplified Langevin model (Pope, 1985),

$$dU_i^{(n)} = - \left( \frac{1}{2} + \frac{3}{4} C_0 \right) \left( U_i^{(n)} - \langle U_i \rangle \right) \frac{dt}{\tau} + (C_0 \epsilon)^{1/2} dW_i, \quad (5)$$

where  $dU_i = U_i(t+dt) - U_i(t)$ , the increment of velocity;  $dt$ , the time increment;  $C_0$ , Kolmogorov constant;  $\epsilon$ , the dissipation rate of the turbulent kinetic energy per unit mass  $k$ ;  $\tau$ , the time scale of turbulence  $\tau = k/\epsilon$ ;  $dW_i$ , the increment of isotropic Wiener process with zero mean and covariance  $\langle dW_i dW_j \rangle = dt \delta_{ij}$ .

### 2.1.3 Molecular Mixing Model

Three fundamental models: the Curl's model (Curl, 1963), the modified Curl's model (Dopazo, 1974; Janika et al., 1979; Pope, 1982) and the binomial Langevin model (Valiño and Dopazo, 1991) are used. Each model is explained in the following.

**Curl's Model** For the Curl's model (Curl, 1963), in the small interval  $dt$  the probability of the  $n$ th particle being mixed is given by

$$P^{(n)} = \frac{2C_\phi dt}{\tau(\mathbf{x}^{(n)}(t))}, \quad (6)$$

where  $C_\phi = \tau/\tau_\phi$  is the empirical constant and  $\tau_\phi$  is the time scale of molecular mixing. When the mixing takes place with this probability, the pair to the  $n$ th particle is selected (here, the  $m$ th particle) and the concentrations of two particles are replaced by their mean:

$$\Gamma_\alpha^{(n)}(t+dt) = \Gamma_\alpha^{(m)}(t+dt) = \frac{1}{2} \left( \Gamma_\alpha^{(n)} + \Gamma_\alpha^{(m)} \right), \quad (7)$$

where the right-hand side of Eq.(7) represents the state at time  $t$ . The nearest stochastic particle is selected as a pair because mixing takes place locally in the physical space.

**Modified Curl's Model** In the modified Curl's model (Dopazo, 1979; Janicka et al., 1979; Pope, 1982), the probability of the particle being mixed is modified by

$$P^{(n)} = \frac{3C_\phi dt}{\tau(\mathbf{x}^{(n)}(t))}, \quad (8)$$

and the concentrations of pair particles are replaced by

$$\Gamma_\alpha^{(n)}(t + dt) = (1 - \beta)\Gamma_\alpha^{(n)} + \frac{1}{2}\beta(\Gamma_\alpha^{(n)} + \Gamma_\alpha^{(m)}), \quad (9a)$$

$$\Gamma_\alpha^{(m)}(t + dt) = (1 - \beta)\Gamma_\alpha^{(m)} + \frac{1}{2}\beta(\Gamma_\alpha^{(n)} + \Gamma_\alpha^{(m)}), \quad (9b)$$

where  $\beta$  is a random variable uniformly distributed on the interval  $[0,1]$ .  $\beta$  represents the degree of mixing in a particle pair; no mixing occurs with  $\beta = 0$ , and the Curl's model is recovered with  $\beta = 1$ .

**Binomial Langevin Model** Valiño and Dopazo (1991) proposed the following binomial Langevin model,

$$d\Gamma^{(n)} = -\frac{1}{2} \left[ 1 + K \left( 1 - \frac{\langle \gamma'^2 \rangle}{\gamma_*'^2} \right) \right] \frac{C_\phi}{\tau} (\Gamma^{(n)} - \langle \Gamma \rangle) dt + \left[ K \left( 1 - \frac{(\gamma'^{(n)})^2}{\gamma_*'^2} \right) \frac{C_\phi}{\tau} \langle \gamma'^2 \rangle dt \right]^{1/2} \xi_{\text{bin}}, \quad (10)$$

where  $K$ , a constant;  $\xi_{\text{bin}}$ , a normalized binomially distributed random variable; and the prime represents the fluctuation value.  $\gamma_*'$  is equal to  $\gamma'_{\text{max}}$  if  $\gamma'^{(n)}$  is positive and equal to  $\gamma'_{\text{min}}$  if  $\gamma'^{(n)}$  is negative, where subscripts max and min are the allowable maximum and minimum fluctuation, respectively.  $\xi_{\text{bin}}$  is generated to preserve the boundedness of the scalar concentration.

#### 2.1.4 Position and Chemical Reaction

The position of the stochastic particles in the physical space and the chemical source term are treated without modeling. This is an advantage in the Lagrangian PDF method used in this study. Therefore, the changes of position and concentration by the chemical reaction are calculated as follows,

$$dx_i = U_i dt, \quad (11)$$

$$d\Gamma_\alpha = w_\alpha dt. \quad (12)$$

## 2.2 Simulation Conditions

Figure 1 shows a schematic diagram of the reactive-scalar mixing layer simulated in this study. Nonpremixed species A and B are supplied from the upstream of the grid with the mesh size of  $M$ , at the constant velocity  $\bar{U}$ . The initial concentrations of species A and B are  $\Gamma_{A0}$  and  $\Gamma_{B0}$ , respectively. The second order and irreversible chemical reaction:



has occurred in the mixing region of species A and B, where species P is produced in the downstream of the grid. The experiments of Komori et al.(1993, 1994) were conducted under

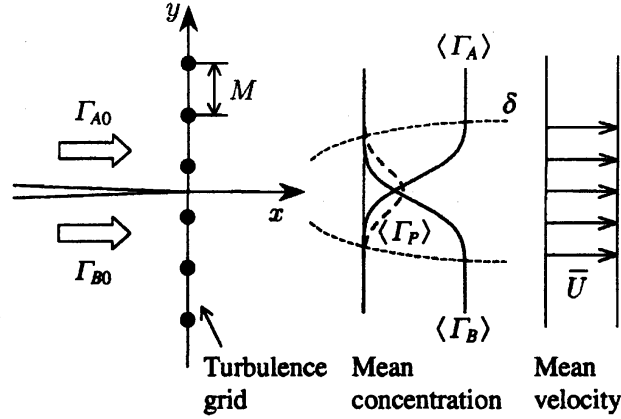


Figure 1: Schematic diagram of the reactive-scalar mixing layer

the following conditions:  $M = 2$  cm and  $\bar{U} = 25$  cm/s, so the mesh Reynolds number  $Re_M = M\bar{U}/\nu = 5000$ .

This problem is two dimensional because of the homogeneity of PDF along the spanwise direction. The longitudinal and transverse coordinates are denoted by  $x$  and  $y$ , respectively, and the corresponding velocity  $\mathbf{U} = (U_x, U_y)$ .

We assume the equal diffusivities for all species and calculate the mixture fraction  $F$  and the concentration of product P, i.e.,  $\mathbf{\Gamma} = (F, \Gamma_P)$ . The mixture fraction is a conserved scalar. The following relation between  $\Gamma_A$ ,  $\Gamma_B$ ,  $\Gamma_P$ , and  $F$  is derived by using the conserved scalar theory (Bilger et al., 1991),

$$\Gamma_A - \Gamma_B = F(\Gamma_{A0} + \Gamma_{B0}) - \Gamma_{B0}, \quad (14a)$$

$$\Gamma_A + \Gamma_P = F\Gamma_{A0}, \quad (14b)$$

$$\Gamma_B + \Gamma_P = (1 - F)\Gamma_{B0}. \quad (14c)$$

Then, using Eqs.(14b) and (14c),  $\Gamma_A$  and  $\Gamma_B$  are calculated from  $F$  and  $\Gamma_P$ . For details of this method in the binomial Langevin model, refer to Hulek and Lindstedt (1995).

Hereafter, all variables in Section 2 are normalized by  $M$ ,  $\bar{U}$ ,  $\Gamma_{A0}$ , and  $\Gamma_{B0}$ . The Damköhler number, that represents the ratio of the time scale of flow to one of chemical reaction, is defined as

$$Da = \frac{Mk_R(\Gamma_{A0} + \Gamma_{B0})}{\bar{U}}, \quad (15)$$

where  $k_R$  is the reaction rate constant. The stoichiometric value of mixture fraction,  $F_S$ , is given by

$$F_S = \frac{\Gamma_{B0}}{\Gamma_{A0} + \Gamma_{B0}}. \quad (16)$$

In the simplified Langevin model for the velocity, either  $\epsilon$  or  $\tau$  must be modeled. In this study, it is assumed that the time scale  $\tau$  is constant in the  $y$ -direction. In the experiment of Komori et al. (1993), it is known that the decay of turbulent intensities are given by

$$\langle u_x'^2 \rangle = \langle u_y'^2 \rangle = 0.0556x^{-1.59}, \quad (17)$$

so here  $\tau$  is modeled to increase linearly in the downstream direction:

$$\tau = \frac{k}{\epsilon} = \left( \frac{3}{2} \langle u_x'^2 \rangle \right) / \left( -\frac{3}{2} \frac{d\langle u_x'^2 \rangle}{dx} \right) = 0.629x. \quad (18)$$

Kolmogorov constant can be related to the turbulent diffusion coefficient through the Lagrangian time scale  $T_L$ :

$$T_L = \frac{4}{3C_0} \tau. \quad (19)$$

Kolmogorov constant is assumed to be  $C_0 = 1.1$  in such a way that the mixing layer thickness agrees with the experimental data. It is smaller than the value used by Pope (1985),  $C_0 = 2.1$ , probably because the Reynolds number of the experiments by Komori et al. (1993, 1994) is rather small.

The empirical constant,  $C_\phi$ , is adjusted to be 0.44 in such a manner as the decay of concentration fluctuation agrees with the experimental data. Although we assume that  $C_\phi$  is constant, it is known that the value of  $C_\phi$  depends on the modeling of molecular mixing time scale  $\tau_\phi$ . For example, using Corrsin's model (1964),  $C_\phi$  varies in the downstream direction and its value is between 0.5-0.6 in the simulation region. Recently, Pipino and Fox (1994) proposed the spectral relaxation model and showed its advantage.

According to Valiño and Dopazo (1991),  $K = 2.1$  is chosen in the binomial Langevin model for the concentration. The simulation has been made for the finite Damköhler number,  $Da = 0.752$ , corresponding to the moderately fast reaction in the experiment of Komori et al. (1994) ( $k_R = 0.047 \text{ m}^3/(\text{mol} \cdot \text{s})$ ,  $\Gamma_{A0} = \Gamma_{B0} = 100 \text{ mol/m}^3$ ).

The frozen limit ( $Da \rightarrow 0$ , corresponding to no reaction) and equilibrium limit ( $Da \rightarrow \infty$ , corresponding to the instantaneous reaction) are determined by using the conserved scalar theory (Bilger et al., 1991) as follows.

As  $Da \rightarrow 0$ ,

$$\lim_{Da \rightarrow 0} \Gamma_A = F, \quad (20)$$

$$\lim_{Da \rightarrow 0} \Gamma_B = 1 - F. \quad (21)$$

As  $Da \rightarrow \infty$ ,

$$\lim_{Da \rightarrow \infty} \Gamma_A = \frac{F - F_S}{1 - F_S} H(F - F_S), \quad (22)$$

$$\lim_{Da \rightarrow \infty} \Gamma_B = \frac{F_S - F}{F_S} H(F_S - F). \quad (23)$$

where  $H$  is the Heaviside unit step function.

The solution in the domain  $2 \leq x \leq 20$ ,  $-2.5 \leq y \leq 2.5$  is calculated by a marching solution method (Pope, 1985). In this method, the constant spatial increment,  $dx = 1/100$ , is related to the time increment of stochastic particle,  $dt^{(n)} = dx/U_x^{(n)}$ . The number of stochastic particles is  $N = 400,000$  and various expectations are calculated in the small region,  $dy = 0.1$ .

With regard to the initial conditions, the stochastic particles are uniformly distributed in the  $y$ -direction at  $x = 2$ , the velocities of them are generated as Eq.(17) is satisfied, and concentrations of them are set to be,

$$\Gamma_A = 1, \quad \Gamma_B = 0, \quad \text{for } y > 0 \quad (24a)$$

$$\Gamma_A = 0, \quad \Gamma_B = 1. \quad \text{for } y < 0 \quad (24b)$$

For the boundary condition, we adopt a perfect reflection of stochastic particles at  $|y| = 2.5$ .

### 2.3 Simulation Result

First, we verify whether the velocity field is simulated correctly by using Eq.(18). Figure 2 shows the simulated decay of turbulent intensities, together with the experimental data by Komori et al. (1993). It is found that the turbulent intensities show good agreements with the experimental data and that the velocity field is simulated correctly.

Figure 3 shows the downstream variations of the mean concentration of species A,  $\langle \Gamma_A \rangle$ , on the centerline ( $y = 0$ ).  $\langle \Gamma_A \rangle$  decreases in the downstream direction for  $Da = 0.752$  and  $Da \rightarrow \infty$  because of the chemical reaction, while for  $Da \rightarrow 0$  it is constant and equal to 0.5. All models show good agreements with the experimental data. However, we find that the Curl's model overestimates the effect of the chemical reaction, probably because the mixing effect of the stochastic particles by the Curl's model is larger than the actual one.

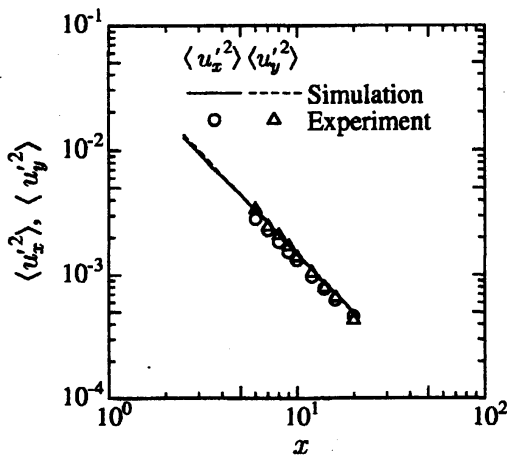


Figure 2: Decay of turbulent intensities

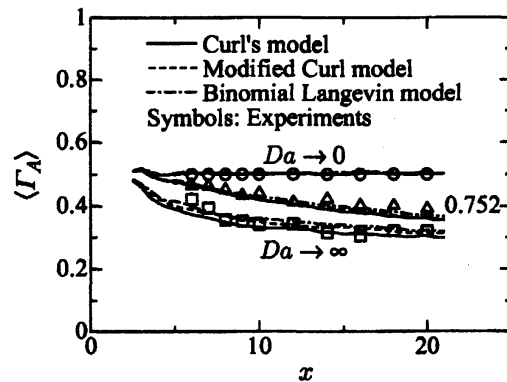


Figure 3: Mean concentration of species a on the centerline (experiments:  $\circ$ , No reaction;  $\triangle$ , Moderately fast reaction;  $\square$ , Instantaneous reaction. Same symbols are used in following figures.)

Figure 4 shows the downstream variations of the mean concentration of product P,  $\langle \Gamma_P \rangle$ , on the centerline. It is also found that the Curl's model overestimates the effect of the reaction.

Transverse profiles of the mean concentration of species A at  $x = 12$  are shown in Fig. 5. The results for  $Da = 0.752$  is not shown in the figure, because there are no experimental data, but these lie between the limits of  $Da \rightarrow 0$  and  $Da \rightarrow \infty$ . In reacting flows, the mean concentration of species A is smaller than the non-reacting flow and the profiles become asymmetric because of the chemical reaction.

Figure 6 shows the concentration fluctuation intensity of species A,  $\langle \gamma_A'^2 \rangle$ , on the centerline. The values of  $\langle \gamma_A'^2 \rangle$  for  $Da \rightarrow \infty$  are larger than those for  $Da \rightarrow 0$ , since species A is consumed by the chemical reaction. The modified Curl's model and binomial Langevin model show good agreements with the data, while the Curl's model gives larger values than those of experiment for  $Da \rightarrow \infty$ . The modified Curl's model shows larger value than the binomial Langevin model, especially near the grid. In the Curl's model and modified Curl's model, the concentrations of stochastic particles are mixed with the probability given by Eq.(6) and Eq.(8), respectively, and the other particles preserve their concentrations. Therefore, the particles that have not been mixed (i.e.,  $\Gamma_A = 1$ ) exist and they make the fluctuation intensity larger in the reacting flow.

The profiles of concentration fluctuation r.m.s. value of species A at  $x = 12$  are shown in

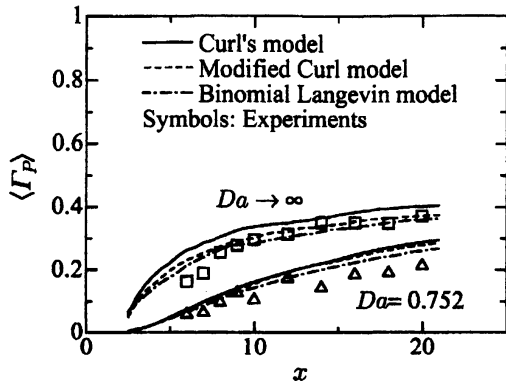


Figure 4: Mean concentration of product P on the centerline

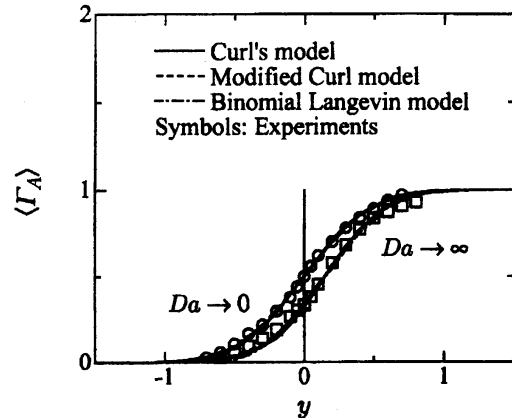


Figure 5: Mean concentration profiles of species A at  $x = 12$ .

Fig. 7. For  $Da \rightarrow \infty$ , the r.m.s. value gives the peak in the region  $y > 0$ , where the reactant A exists in excess, and the peak value becomes larger than one for  $Da \rightarrow 0$  by the effect of the chemical reaction. The Curl's model and modified Curl model show larger value than the binomial Langevin model in the region  $y < 0$  for  $Da \rightarrow \infty$ . It is probably caused by the effect of the particles that have not been mixed.

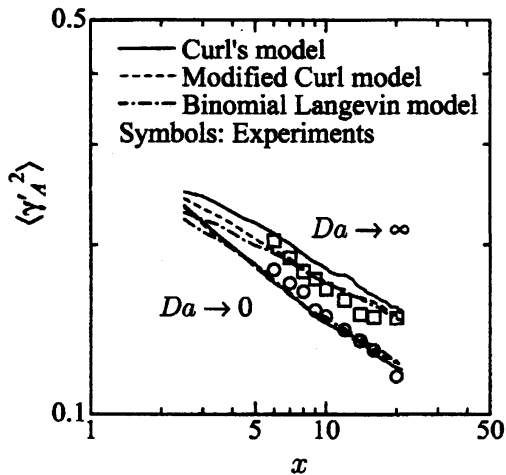


Figure 6: Concentration fluctuation intensity of species A on the centerline

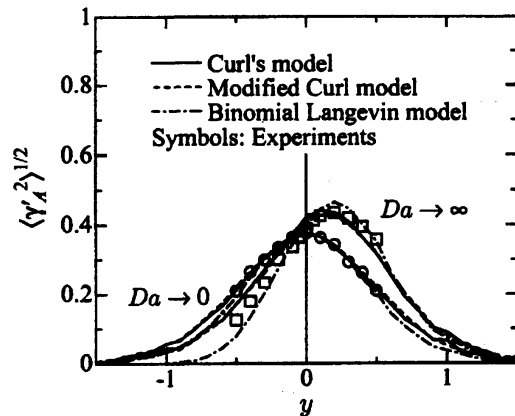


Figure 7: Profiles of concentration fluctuation r.m.s. value of species A at  $x = 12$ .

Figure 8 shows the concentration correlation coefficient between species A and B,  $R_{AB}$ , on the centerline.  $R_{AB} = 1$  in the case of  $Da \rightarrow 0$ , since concentration fluctuation  $\gamma'_A = -\gamma'_B$ .  $R_{AB}$  increases in the downstream direction by the chemical reaction. It is found that the Curl's model overestimates the effect of the reaction and that the modified Curl's model and binomial Langevin model show good agreements with the experimental data.

Figure 9 shows the segregation coefficient,  $\alpha = \langle \gamma_A \gamma_B \rangle / (\langle \Gamma_A \rangle \langle \Gamma_B \rangle)$ , on the centerline.  $\alpha$  indicates the degree of the coexistence between species A and B. We can easily find  $\alpha = 0$  if species are mixed completely, and  $\alpha = -1$  if there is no mixing. For  $Da \rightarrow 0$ ,  $\alpha$  increases gradually, because the mixing proceeds in the downstream. For  $Da \rightarrow \infty$ ,  $\alpha = -1$ , since

the reaction is instantaneous, so that species A and B can not be coexisted. The calculated values by all models agree well the experiments for  $Da \rightarrow 0$  and  $Da \rightarrow \infty$ . For  $Da = 0.752$ , the experiment shows the increase of  $\alpha$  in the downstream, while the simulation gives some decreasing of  $\alpha$  in the region  $x > 8$ . But we find the difference among three models is relatively small.

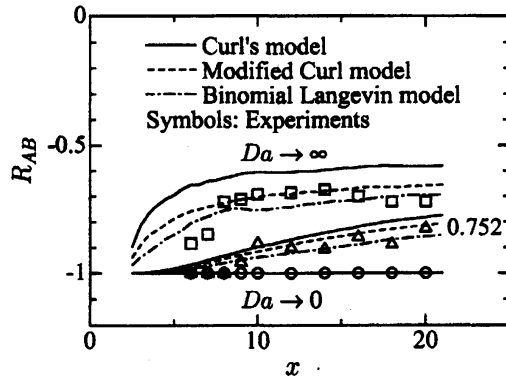


Figure 8: Correlation coefficient on the centerline

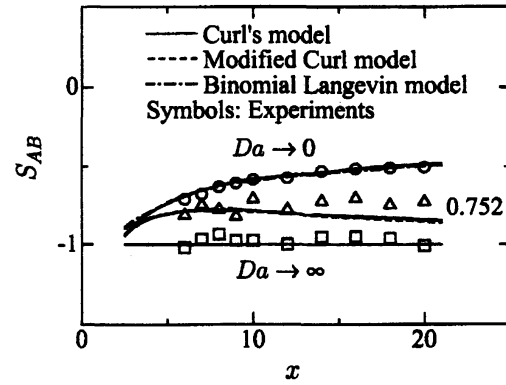


Figure 9: Segregation coefficient on the centerline

## 2.4 Conclusions of Section 2

The reactive-scalar mixing layer in a grid-generated turbulence is studied numerically by the Lagrangian PDF method. Main conclusions are as follows.

- (1) The simulation results of the mean concentration, the concentration fluctuation, and the concentration covariance show good agreements with the experimental data as a whole. So, the PDF calculation is valid for the liquid phase by adjusting the model constant.
- (2) The Curl's model tends to overestimate the effect of the chemical reaction. However, the modified Curl's model and the binominal Langevin model can overcome this defect.

## 3 Axisymmetric Point Source Plume Diffusion in a Turbulent Pipe Flows (Problem (B))

Now we move to the problem (B): the axisymmetric point source plume in a fully developed turbulent pipe flow.

### 3.1 Coordinate System

Here, the coordinate system  $(r, \theta, x)$  is used as shown in Fig.10, where  $r, \theta, x$  are the radial, azimuthal and main streamwise coordinate, respectively.  $R$  is the inner radius of the pipe.

### 3.2 Conditions of the Lagrangian Velocity Model

For the simulation of velocity field, the semiempirical Lagrangian stochastic model is adopted to save the computing time and improve the efficiency of the algorithm. At first, we assume that the evolutions of the moments of Euler velocity pdf in a pipe flow (the first and second moment etc.) are known from the experimental data, then the generalized Langevin equation

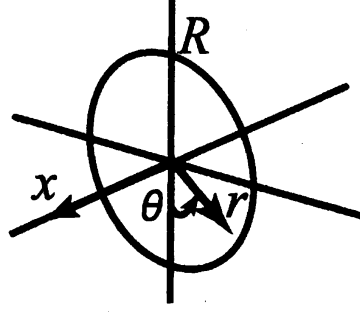


Figure 10: Coordinate system

is constructed so that the evolutions of the moments calculated by the model may be equal to those (the consistency condition (Pope, 1987)). Another important condition for the stochastic model is the so-called “thermodynamic constraint” that an initially uniform distribution of material be maintained (Sawford, 1986). In other words, if, initially, the number density of marked stochastic particles is uniform, then it remains uniform. According to Pope (1987), the above condition is equivalent to the condition that the calculated mean velocity satisfies the continuity equation.

### 3.3 A Generalized Langevin Model in the Cylindrical Coordinates

In the present study, the motion of fluid particle is modeled and tracked by the generalized Langevin model. Here we show only the equations used (See Sakai et al. (1996) for details).

Assuming axisymmetry and the condition of full development for the turbulent pipe flow, we can derive the following final form of the generalized Langevin model for each velocity component,

$$dU_r^* = -\frac{1}{\rho} \frac{\partial \bar{P}}{\partial r} dt + \frac{1}{r^*} U_{\theta}^{*2} dt + G_{rr} U_r^* dt + G_{rx} (U_x^* - \bar{U}_x) dt + \sqrt{C_0 \varepsilon} dW_r, \quad (25a)$$

$$dU_{\theta}^* = -\frac{U_r^* U_{\theta}^*}{r^*} dt + G_{\theta\theta} U_{\theta}^* dt + \sqrt{C_0 \varepsilon} dW_{\theta}, \quad (25b)$$

$$dU_x^* = -\frac{1}{\rho} \frac{\partial \bar{P}}{\partial x} dt + \nu \frac{1}{r^*} \frac{d}{dr} \left( r^* \frac{d\bar{U}_x}{dr} \right) dt + G_{rr} U_r^* dt + G_{xx} (U_x^* - \bar{U}_x) dt + \sqrt{C_0 \varepsilon} dW_x, \quad (25c)$$

where \* denotes the random variable attendant on the particle,  $dt$ : the time increment,  $dU_i$ : the increment of velocity component ( $i = r, \theta, x$ ),  $\varepsilon$ : mean dissipation rate per unit mass,  $C_0$ : Kolmogorov constant,  $dW_i$ : increment of an isotropic Wiener process in the  $i$  direction with the mean 0 and variance 1. The tensor  $G_{ij}$  is determined on the basis of the consistency condition (Pope, 1987) up to the second-order moments of the velocity field (See Sakai et al. (1996) for details on  $G_{ij}$ ). And the gradient of the mean pressure can be expressed as

$$\frac{1}{\rho} \frac{\partial \bar{P}}{\partial r} = -\frac{1}{r} \frac{\partial}{\partial r} (r \overline{u_r^2}) + \frac{\overline{u_{\theta}^2}}{r}, \quad (26)$$

$$\frac{1}{\rho} \frac{\partial \bar{P}}{\partial x} = -2 \frac{\overline{u_r^2}}{R}. \quad (27)$$

Here, to satisfy consistency condition up to the second-order moments of the velocity, it is

necessary to specify the radial distributions of the following mean quantities up to the third-order.

First-order moment	:	$\overline{U_x}$
Second-order moments	:	$\overline{u_r^2}, \overline{u_\theta^2}, \overline{u_x^2}, \overline{u_r u_x}$
Third-order moments	:	$\overline{u_r^3}, \overline{u_r^2 u_x}, \overline{u_r u_\theta^2}, \overline{u_r u_x^2}, \overline{u_\theta^2 u_x}$
mean dissipation rate per unit mass	:	$\varepsilon$

In the following, we explain the way of giving these parameters. Firstly, the radial distribution of the mean velocity is given by the following equation in which the wake function (Tennekes and Lumley, 1972) is added to the equation of mean velocity by Reichardt (See Hinze, 1975),

$$\begin{aligned} \frac{\overline{U_x}}{u_r} &= \frac{1}{\kappa} \ln(1 + \kappa y^+) + c \left[ 1 - \exp\left(-\frac{y^+}{\delta_l^+}\right) - \frac{y^+}{\delta_l^+} \exp(-0.33y^+) \right] \\ &+ d \left[ 1 - \cos\left(\pi \frac{y}{\delta}\right) \right], \\ \kappa &= 0.4, \quad c = 6.0, \quad \delta_l^+ = 11.0, \quad d = 0.5, \quad \delta = 0.77R, \end{aligned} \quad (28)$$

where  $y^+ = u_r y / \nu$  ( $y$ : distance from the wall;  $y = R - r$ ) and the third term of the right-hand side is the wake function. The parameters  $c$  and  $\delta$  are chosen for the mean velocity at the center of the pipe  $\overline{U_c}$  and the cross-sectional mean velocity  $U_{av}$  to agree with those given by Becker et al. (1966). The experimental study by Becker et al. is the subject of the simulation in the present research.

With regard to the second-order moments, i.e.  $\overline{u_r^2}, \overline{u_\theta^2}$  and  $\overline{u_x^2}$  and the mean dissipation rate  $\varepsilon$ , Laufer(1954)'s data (Reynolds number  $Re_c = 2R\overline{U_c}/\nu = 500,000$ ) are used. Here it is noted that the Reynolds number of Laufer's experiment is different from that of the experiment by Becker et al. (1966) ( $Re_c = 2R\overline{U_c}/\nu = 796,000$ ; This value corresponds to  $Re = 2RU_{av}/\nu = 684,000$ ). However, both  $Re_c$  are in the same order, so distributions of the second moments and the mean dissipation rate are not so different with each other. From this reason, the Laufer's experimental results are used as the specified data.

The Reynolds stress  $\overline{u_r u_x}$  is readily determined by integrating the  $x$ -direction mean velocity equation, which is given by

$$\overline{u_r u_x} = \nu \frac{\partial \overline{U_x}}{\partial r} + \frac{u_r^2}{R}. \quad (29)$$

With regard to the third-order moments of the velocity, although there exist Laufer's experimental data, the scattering of the data is quite large. Thus, we judged that those data are not suitable for inputting to the present model, and decided to omit the input of the third-order moments to the model. This means that the present model does not satisfy the consistency condition exactly. Thus we need to check the consistency condition in the practical simulation in order to judge whether the present model gives us reliable results or not. This check is made by comparing the calculated statistics of the velocity field with the experimental (prescribed) data.

### 3.4 Molecular Mixing Model

In the present problem, the Dopazo(1975)'s deterministic model and the modified Curl's model(Dopazo, 1975; Janicka et al, 1979; Pope, 1982) are adopted as the molecular mixing

model. The modified Curl's model has been already explained in §2.1.3. In the following, we explain the Dopazo's model.

### 3.4.1 Dopazo's Deterministic Model.

In the Dopazo's deterministic model (Dopazo, 1975), when the scalar (concentration) attendant on the particle is represented by  $\Gamma$ , the increment of the scalar  $d\Gamma$  is given by

$$d\Gamma = -\frac{1}{2}C_\phi(\Gamma - \langle\Gamma\rangle)\frac{dt}{\tau}, \quad (30)$$

where  $\langle\Gamma\rangle$  is the ensemble average of the scalar over particles within each cell which is fixed on the spatial area.  $C_\phi$  is the parameter which determines the decay rate of the variance of the scalar. And  $\tau$  is the turbulent time scale, which is defined by

$$\tau = \frac{\kappa}{\varepsilon}, \quad \kappa = \frac{\overline{u_r^2} + \overline{u_\theta^2} + \overline{u_x^2}}{2}, \quad (31)$$

where  $\kappa$  is the turbulent kinetic energy,  $\varepsilon$  is the dissipation rate of  $\kappa$ . In this model, the scalar attendant on the particle is determined not randomly but deterministically.

## 3.5 Simulation Conditions

The subject of the present simulation is the oil fog diffusion field by Becker et al. (1966). The simulation conditions are adjusted to those of the experiments by Becker et al.. In the experiments, the measurements of the concentration field of the point source plume of oil fog which is injected from the center of the pipe in a fully developed turbulent pipe flow were made. The fog injector's inner diameter is 2.16 mm, and the outer diameter is 2.77 mm. In the actual experiments, the measurement points were fixed and the injector was moved, then the concentrations were measured at the several downstream cross sections from the injector's exit (the plume source). On the other hand, we fixed the plume source at the origin and calculated concentrations at the same downstream distances from the source as those of experiments. Further, Becker et al. performed the experiments for several values of  $\overline{U_c}$ , but in this study we chose only one case of these experiments as the simulation subject: the case of  $\overline{U_c}=61$  m/s ( $Re=684,000$ ). The conditions of the simulation are as follows.

inner radius of the pipe	: $R = 0.1005$ m
cross-sectional mean velocity	: $U_{av} = 52.38$ m/s
kinematic viscosity	: $\nu = 1.54 \times 10^{-5}$ m <sup>2</sup> /s
Reynolds number	: $Re = 2RU_{av}/\nu = 684,000$
friction velocity	: $u_\tau = 2.15$ m/s
Kolmogorov constant	: $C_0 = 2.0$
boundary condition	: absorptive wall

## 3.6 Simulation Results

### 3.6.1 Verification of the Velocity Field

Firstly, we made the numerical verifications of the consistency condition (Pope, 1987) up to the second-order moment and the thermodynamic constraint (Sawford, 1986) for the calculated velocity field. Since the subject of calculation is a fully developed turbulence field and

the velocity field is independent of the azimuthal-direction, only the radial movements of the particles were calculated in this verification. Although the figures are not shown here because of the limitation of the paper length, it was confirmed that the velocity field simulated by the present model can reproduce well the prescribed data up to the second-order moment even if the input of the third-order moment is omitted. This gives us some practical background to rely on the simulation of the scalar diffusion problem shown in the following section. Further, it was also ascertained that the initial uniform distribution of stochastic particles is almost unchanged with time in the simulation. Thus we concluded that the velocity field simulated by the present model satisfies the thermodynamic constraint, i.e., the continuity condition (Sawford, 1986).

### 3.6.2 Scalar Diffusion from the Center of the Pipe

For the simulation of the scalar field, the two-dimensional calculation of the radial and main streamwise direction was made because of the axisymmetry of the pipe. Thus, the distance of the particle movement in the radial and main streamwise direction  $dr^*$ ,  $dx^*$  during the time increment  $dt$  is calculated by

$$dr^* = U_r^* dt, \quad (32)$$

$$dx^* = U_x^* dt. \quad (33)$$

First, at the initial time the particles are distributed uniformly over the area of the calculation ( $r = 0 \sim R, x = 0 \sim 7.0R$ ) and the particles within the source are given the scalar value of 1, the others are given the scalar value of 0. The change of the scalar attendant on each particle is calculated by the molecular mixing model mentioned in the previous section. The size of the source is  $0.04R$  in both the radial direction and the main streamwise direction. This size was determined on the basis of the empirical equation of the mixing length given by Nikuradse (see Schlichting, 1979). The total number of particles is  $N_t = 2,000,000$ , the time increment is  $dt = 4.67 \times 10^{-6}$  sec for one step, and the total number of time steps is 11,000, which corresponds to the real time of  $5.137 \times 10^{-2}$  sec. The parameter  $C_\phi$ , which determines the decay rate of the variance of the scalar, is 7.5. In order to calculate the statistics of scalar diffusion field, we take the ensemble average over particles within each spatially discretized cell which is distributed in the radial and main streamwise direction. The total number of cells of radial direction is 40 and the width of the  $k$ th cell  $\Delta r^{(k)}$  from the center of the pipe is given by

$$\Delta r^{(k)}/R = -a(k-1) + 0.04, \quad (34)$$

where the constant  $a$  is 0.00076923 which is chosen so that the summation of the width of each cell becomes  $R$ . With regard to the cells of the main streamwise direction, their widths are constant with  $\Delta x^{(m)}/R = 0.04$  ( $m$  means the  $m$ th cell) and the total number is 175. In the following, the simulation results are shown.

Figure 11 shows the radial profiles of the mean concentration. In this figure, the ordinate is normalized by the maximum of mean concentration in each cross-section  $\bar{\Gamma}_{max}$  and the abscissa by concentration half-radius of plume  $r_{1/2}$ . The lines show the simulation results by two molecular mixing models (i.e., the Dopazo's deterministic model and the modified Curl's model) and the symbols show experimental data by Becker et al. (1966). From this figure, it is found that both simulation results agree with experimental data as a whole.

Figure 12 shows the radial profiles of the r.m.s value of concentration fluctuations. In this figure, the lines show the simulation results by two molecular mixing models and the symbols show the experimental data by Becker et al.. The ordinate is normalized by the maximum of

mean concentration in each cross-section  $\bar{\Gamma}_{max}$  and the abscissa by  $r_{1/2}$ . From the figure, it is found that the difference by the mixing models is not so large, and the whole shape of any simulated distribution almost agrees with the experimental one.

Figure 13 shows the main streamwise variation of the scalar PDF on the centerline of the pipe. Figs.(a),(b) show the simulation results by the Dopazo's deterministic model and the modified Curl's model, respectively. In these figures, the range  $[0, 1]$  which the scalar value can take is divided into one hundred pieces. From these figures, it is found that the modified Curl's model has the larger effect of the molecular mixing than the Dopazo's model: the PDF profile by the modified Curl's model shows the two large spikes near  $\Gamma = 0$  and  $\Gamma = 1$  at the upstream region (at  $x/R = 1.99$ ), but as going to the downstream direction the uniformization of the concentration (molecular mixing) has proceeded rapidly, then at the downstream region (at  $x/R = 4.54$ ) the PDF shows the monotonously decreasing profile from the peak near  $\Gamma = 0$  to the small value at the large concentration region, while in the PDF profile by the Dopazo's model the two peaks remain at the downstream region because of the less effect of molecular mixing. This difference of molecular mixing effect between the two models seems to be worth consideration to make the prediction of other diffusion fields by the PDF method in the future. Further, although the figures are not shown here, it has been ascertained that both models gives almost the same downstream variations of the mean concentration and the r.m.s. value of concentration (i.e., the first-order and the second-order moment of the PDF). Consequently it is found that both mixing models can express well the characteristics of the mixing process at least up to the second-order moment of the scalar PDF in the plume.

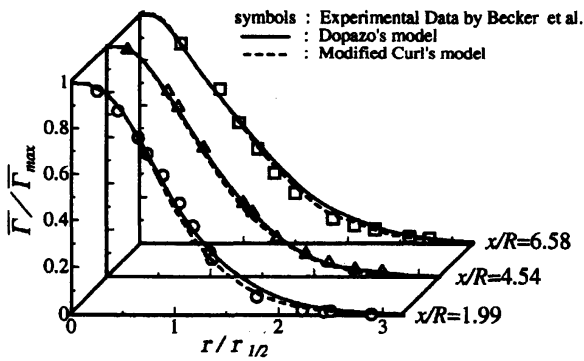


Figure 11: Radial profiles of the mean concentration

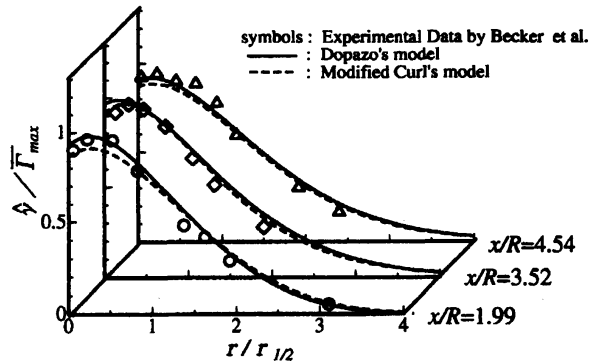
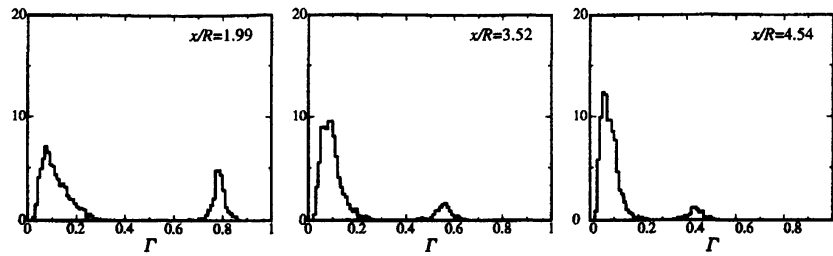


Figure 12: Radial profiles of the r.m.s value of concentration fluctuations

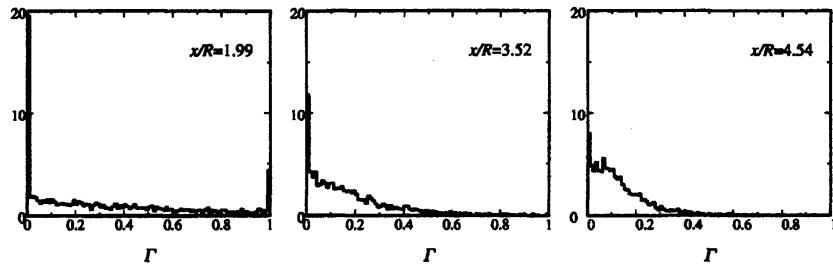
### 3.7 Conclusions of Section 3

The axisymmetric point source plume in a fully developed turbulent pipe flow is studied numerically by the Lagrangian PDF method. The conclusions obtained in this section are as follows.

- (1) From the simulation results of the diffusion field from the source at the center of the pipe, it was found that the radial profiles of the mean concentration and concentration fluctuation r.m.s value by two molecular mixing models (the Dopazo's model and the modified Curl's model) show good agreement with experimental data as a whole.
- (2) From the downstream variations of the scalar pdf profiles, it was found that the modified Curl's model has the larger mixing effect than the Dopazo's model, but the downstream variations of the scalar PDF profiles by both mixing models can characterize well the mixing process of the scalar plume from the point source on the center line of the pipe.



(a) Dopazo's model



(b) Modified Curl's model

Figure 13: Downstream variation of the scalar PDF profile

## 4 Summary

The Lagrangian PDF method is a kind of Monte-Carlo method in which the modeled equations for the velocity and scalar of stochastic particle are constructed and they are solved numerically by integrating the state of stochastic particles under the given initial conditions and boundary conditions for the problems. In this study, the Lagrangian PDF method was applied to the two mixing layer problems, i.e., the problem (A) : the reactive-scalar mixing layer of liquid phase in grid-turbulence; the problem (B) : the axisymmetric turbulent plume diffusion in a pipe flow.

For the velocity of the stochastic particles, the simplified Langevin model and the generalized Langevin model were used for the problem (A) and (B), respectively. With regard to the molecular mixing model, three models (the Curl's model, the modified Curl's model and the binomial Langevin model) were adopted for the problem (A), and two models (the Dopazo's model and the modified Curl's model) were used for the problem (B). The simulation results were compared with the experimental data by Komori et al. (1993, 1994) for the problem (A) and by Becker et al. (1966) for the problem (B).

Consequently, it was confirmed that the present simulation method is valid to predict the distributions of the moments of the scalar PDF at least up to the second-order if the molecular mixing models are appropriately chosen. However, we do not make sure yet whether the present simple velocity and molecular mixing models give the correct results for the higher-order moments of the scalar PDF. In the future, the usefulness of the present models will be examined for other complicated diffusion processes and reactive flows, e.g., in the turbulent jet, in the turbulent boundary layer and in the turbulence around the bluff body, etc.. Finally, it should be noted that more recently other mixing models have been suggested, e.g., a mapping closure model (Chen et al., 1989) and the spectral relaxation model (Pipino and Fox, 1994). However, these new models were complicated in comparison with the simple models used in

this study. The simplicity of the model is a very important factor for the application of the model to the engineering problems. The use of these new models is also our future work.

## Reference

- Becker, H. A., Rosensueing, R. E. and Gwozdz, J. R., 1966, "Turbulent Dispersion in a Pipe Flow," *AIChE J.*, vol.12, No.5, pp.962-972.
- Bilger, R. W., Saetran, L.R., and Krishnamoorthy, L. V., 1991, "Reaction in a Scalar Mixing Layer," *J. Fluid Mech.*, Vol.233, pp.211-242.
- Bilger, R. W., 1993, "Conditional Moment Closure for Turbulent Reacting Flow," *Phys. Fluids*, A Vol.5, pp. 436-444.
- Corrsin, S., 1964, "The Isotropic Turbulent Mixer: Part II. Arbitrary Schmidt Number," *AIChE J.*, Vol.10, pp.870-877.
- Chen, H., Chen, S. and Kraichnan, R.H., 1989, "Probability Distribution of a Stochastically Advected Scalar Field," *Phys. Rev. Lett.*, Vol.63, No.24, pp.2657-2660.
- Curl, R. L., 1963, "Dispersed Phase Mixing: I. Theory and Effects in Simple Reactors," *AIChE J.*, Vol.9, pp.175-181.
- Dopazo, C., 1975, "Probability Density Function Approach for a Turbulent Axisymmetric Heated Jet. Centerline evolution," *Phys. Fluids*, Vol.18, pp.397-404.
- Dopazo, C., 1979, "Relaxation of Initial Probability Density Functions in the Turbulent Convection of Scalar Fields," *Phys. Fluids*, Vol.22, pp.20-30.
- Haworth, D. C. and Pope, S. B., 1986, "A Generalized Langevin Model for Turbulent Flows," *Phys. Fluids*, Vol.29, No.2, pp.387-405.
- Hinze, J.O., 1975, "Turbulence," 2nd ed., McGraw-Hil, New York, p.621.
- Hulek, T., and Lindstedt, R. P., 1995, "Transported Pdf Modelling of Nitric Oxide Conversion in a Mixing Layer," *Proceedings of the 10th Symposium on Turbulent Shear Flows*, Pennsylvania State University, pp.22-7-22-12.
- Janicka, J., Kolbe, W., and Kollmann, W., 1979, "Closure of the Transport Equation for the Probability Density Function of Turbulent Scalar Fields," *J. of Non-Equilibrium Thermodynamics*, Vol.4, pp.47-66.
- Klimenko, A., Yu., 1990, "Multicomponent Diffusion of Various Admixture in Turbulent Flow," *Fluid Dynamics*, Vol.25, pp.327-334.
- Komori, S., Hunt, J. C. R., Kanzaki, T., and Murakami, Y., 1991, "The Effect of Turbulent Mixing on the Correlation between Two Species and on Concentration Fluctuations in Non-Premixed Reacting Flows," *J. Fluid Mech.*, Vol.228, pp.629-659.
- Komori, S., Nagata, K., Kanzaki, T., and Murakami, Y., 1993, "Measurements of Mass Flux in a Turbulent Liquid Flow with a Chemical Reaction," *AIChE J.*, Vol.39, pp.1611-1620.
- Komori, S., Kanzaki, T., and Murakami, Y., 1994, "Concentration Correlation in a Turbulent Mixing Layer with Chemical Reaction," *J. Chem. Eng. of Japan*, Vol.27, pp.742-748.
- Leonard, A. D., Hamlen, R. C., Kerr, R. M., and Hill, J. C., 1995, "Evaluation of Closure Models for Turbulent Reacting Flows," *Ind. & Eng. Chem. Res.*, Vol.34, pp.3640-3652.
- Laufer, J., 1954, "The Structure of Turbulence in Fully Developed Pipe Flows," *NACA Tech.*, Report No.1174.
- Pipino, M., and Fox, R. O., 1994, "Reactive Mixing in a Tubular Jet Reactor: A Comparison of Pdf Simulations with Experimental Data," *Chem. Eng. Sci.*, Vol.49, pp.5229-5241.
- Pope, S.B., 1982, "An Improved Turbulent Mixing Model," *Comb. Sci. and Tech.*, Vol.28, pp.131-145.
- Pope, S.B., 1985, "Pdf Method for Turbulent Reactive Flows," *Prog. Energy. & Comb. Sci.*,

- Vol.11, pp.119-192.
- Pope, S.B., 1987, "Consistency Conditions for Random-walk models of Turbulent Dispersion," *Phys. Fluids*, Vol.30, No.8, pp.2374-2379.
- Pope, S.B., 1994, "Lagrangian PDF Methods for Turbulent Flows," *Ann. Rev. Fluid. Mech.*, Vol.26, pp.23-63.
- Sakai, Y., Nakamura, I., Tsunoda, H. and Hanabusa, K., 1996, "Diffusion in Turbulent Pipe Flow Using a Stochastic Model," *JSME Int. J.*, Series B, Vol.39, No.4, pp.667-675.
- Sawford, B.L., 1986, "Generalized random Forcing in Random-walk Turbulent Dispersion models," *Phys. Fluids*, Vol.29, No.11, pp.3582-3585.
- Slichting, H., 1979, "Boundary-Layer Theory," 7th ed., MacGraw-Hill, New York, pp.604-606.
- Tennekes, H. and Lumley, J. L., 1972, "A First Course in Turbulence," MIT Press., New York, p.162.
- Toor, H. L., 1969, "Turbulent Mixing of Two Species with and without Chemical Reactions," *Ind. & Eng. Chem. Fund.*, Vol.8, pp.655-659.
- Tsai, K., and Fox, R. O., 1994, "Pdf Simulation of a Turbulent Series-Parallel Reaction in an axisymmetric Reactor," *Chem. Eng. Sci.*, Vol.49, pp.5141-5158.
- Valiño, L., and Dopazo, C., 1991, "A Binomial Langevin Model for Turbulent Mixing," *Phys. Fluids*, A Vol.3, pp.3034-3037.